


Little-Parks oscillation and d-vector texture in spin-triplet superconducting rings with bias current

 Kazushi Aoyama 

Department of Earth and Space Science, Graduate School of Science, Osaka University, Osaka 560-0043, Japan

 (Received 19 May 2022; accepted 22 July 2022; published 2 August 2022)

We theoretically investigate the critical bias current j_c for a superconducting (SC) ring in a magnetic field. Based on the Ginzburg-Landau theory, we show that j_c exhibits a Little-Parks (LP) oscillation as a function of the magnetic flux passing through the ring, similarly to the LP oscillation in the SC transition temperature. It is also found that for a spin-triplet SC ring, the \mathbf{d} vector rotates to yield a larger j_c , forming a texture along the circumference of the ring. Experimental implications of our result are discussed.

 DOI: [10.1103/PhysRevB.106.L060502](https://doi.org/10.1103/PhysRevB.106.L060502)

Introduction. In superconductors, a phase of the macroscopic wave function describing the Cooper pair condensate, i.e., a phase of the gap function, often plays an important role for electromagnetic properties of the system. A typical example of such a phase-related phenomenon is the Little-Parks (LP) oscillation emerging in a superconducting (SC) ring in a magnetic field, where the phase and an associated SC current discontinuously change with increasing field, and resultantly, a SC transition temperature T_c exhibits a quantum oscillation as a function of field with its period being characterized by the flux quantum $\Phi_0 = \frac{hc}{2|e|}$ [1–3]. In this Letter, we consider a situation where a bias electric current is further applied to the ring, and theoretically investigate the LP oscillation in the critical bias current j_c at a temperature below T_c . In contrast to the spin-singlet case where only the phase degree of freedom is active, in the spin-triplet case, not only the phase but also the \mathbf{d} -vector degrees of freedom characterizing the three spin states turn out to be essential for j_c .

An experimental setup for the usual LP oscillation in T_c is illustrated in Fig. 1(a). Assuming that the ring width w and thickness d are sufficiently small, the SC gap function for the spin-singlet s -wave pairing is expressed as $\Delta_s = |\Delta|e^{-in\varphi}$ with integer winding number n and azimuthal angle φ . In the presence of an axial magnetic field \mathbf{H} , the SC current circulating around the ring is given by $\mathbf{j} \propto \hat{\varphi}|\Delta|^2(n - \frac{\Phi}{\Phi_0})$ with the magnetic flux passing through the ring Φ [2,4]. Here, the first and second terms in \mathbf{j} originate from the phase gradient and the London screening, respectively. With increasing field, or equivalently, increasing Φ , the integer n switches to a larger value to reduce \mathbf{j} . The occurrence of such a higher- n state and the associated discontinuous change in n are reflected in T_c as the LP oscillation [see Fig. 1(c) and the text below] [1,2,4].

On the other hand, as illustrated in Fig. 1(b), when a bias current is applied to the ring from left to right, the upper and lower halves of the ring are no longer equivalent, and the properties of this current-carrying SC state are not so trivial [5–7]. Furthermore, in a recent LP experiment done on polycrystalline β -Bi₂Pd in this setting, a half-quantum-shifted LP oscillation has been observed and the realization of a spin-triplet SC state has been discussed [8]. In view of such a situation, we theoretically investigate the LP oscillation in the presence of the bias current for both the spin-singlet

and spin-triplet SC rings without any domains and Josephson junctions.

In the LP experiment with the bias current, one usually measures the resistivity which is associated with the critical bias current j_c . In this Letter, we calculate j_c at a low temperature below T_c where the SC gap is well developed. Based on the Ginzburg-Landau (GL) theory, we show that in the spin-triplet case, not only the phase but also the \mathbf{d} vector rotates along the circumference of the ring to yield a larger j_c . To our knowledge, a well-established theory of j_c even for the spin-singlet SC ring is lacking (j_c derived in Refs. [6,7]

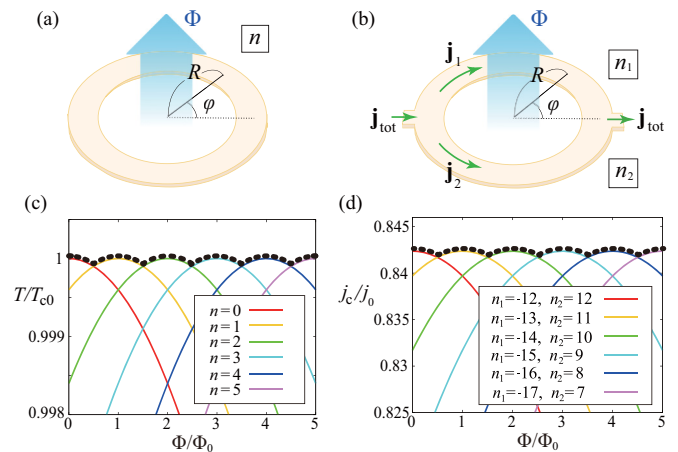


FIG. 1. System setup and the Little-Parks (LP) oscillation. (a) and (b) SC rings of mean radius R involving the magnetic flux Φ in the cases (a) without and (b) with a bias current $\mathbf{j}_{\text{tot}} = \mathbf{j}_1 + \mathbf{j}_2$, where φ denotes an azimuthal angle. In (a), n is a phase winding number for the whole system, whereas in (b), n_1 and n_2 are phase winding numbers in the upper and lower arms of the ring, respectively. (c) Calculated SC transition temperature and (d) critical bias current obtained for the spin-singlet s -wave ring of radius $R/\xi_0 = 50$ in the settings (a) and (b), respectively, where colored curves are obtained for given n 's or sets of n_1 and n_2 , and their largest values are traced by a dotted black curve which exhibits the LP oscillation. (d) is obtained at $T/T_{c0} = 0.6$.

will be discussed later on), so that we shall start from the LP oscillation for the spin-singlet s -wave ring.

Spin-singlet s -wave case. For the bulk singlet s -wave superconductor, the GL free energy \mathcal{F}_{GL} and the SC current \mathbf{j} are derived from the weak-coupling BCS Hamiltonian as $\mathcal{F}_{\text{GL}} = \int d\mathbf{r}[\alpha|\Delta_s|^2 + \beta|\Delta_s|^4 + K|\mathbf{\Pi}\Delta_s|^2]$ and $\mathbf{j} = -\frac{\delta\mathcal{F}_{\text{GL}}}{\delta\mathbf{A}} = -2|e|K(\Delta_s^*\mathbf{\Pi}\Delta_s + \Delta_s\mathbf{\Pi}^\dagger\Delta_s^*)$, where the coefficients are given by $\alpha = N(0)\ln\frac{T}{T_{c0}}$, $\beta = \frac{7\zeta(3)N(0)}{16\pi^2T^2}$, and $K = N(0)(\frac{T_{c0}}{T})^2\xi_0^2$ with density of states at the Fermi level $N(0)$, the SC transition temperature at zero field T_{c0} , and the SC coherence length $\xi_0 = \sqrt{\frac{7\zeta(3)}{48\pi^2}\frac{v_F}{T_{c0}}}$ [9]. For the SC ring with sufficiently small width w and thickness d , the gap function basically depends only on φ , namely, $\Delta_s = |\Delta|e^{-in\varphi}$, and the gauge field can be expressed as $\mathbf{A} = \frac{1}{2}\mathbf{H} \times \mathbf{r} = \frac{HR}{2}\hat{\varphi}$, so that $\mathbf{\Pi} = -i\nabla + 2|e|\mathbf{A}$ is reduced to $\mathbf{\Pi} = \hat{\varphi}\frac{1}{R}(-i\partial_\varphi + \frac{\Phi}{\Phi_0})$ with $\Phi = \pi R^2H$.

By substituting $\Delta_s = |\Delta|e^{-in\varphi}$ into \mathcal{F}_{GL} , one obtains the free-energy density $f_{\text{GL}} = \mathcal{F}_{\text{GL}}/(2\pi Rwd)$ as $f_{\text{GL}} = |\Delta|^2[\alpha + \frac{K}{R^2}(n - \frac{\Phi}{\Phi_0})^2] + \beta|\Delta|^4$. Since the SC transition temperature is determined by the GL quadratic term via the condition $\alpha + \frac{K}{R^2}(n - \frac{\Phi}{\Phi_0})^2 = 0$, it turns out that with increasing Φ , the phase winding number n switches to a larger value to lower the gradient energy $\frac{K}{R^2}(n - \frac{\Phi}{\Phi_0})^2$. The calculation result for $R/\xi_0 = 50$ is shown in Fig. 1(c). One can see that the highest transition temperature indicated by a dotted curve in Fig. 1(c) exhibits a quantum oscillation with its period being characterized by Φ_0 , i.e., the LP oscillation. We note in passing that roles of larger w and d have been discussed elsewhere [3,10]. Also, in quantum-wire systems where electrons are confined in nanostructures, a ring shape seems to be important [11], but such a shape effect should be irrelevant in the present LP system with $w, d \gtrsim \xi_0$.

In the case with the bias current shown in Fig. 1(b), the phases in the upper and lower arms of the ring are not necessarily the same, so that we assume

$$\Delta_s = |\Delta| \begin{cases} e^{-in_1\varphi} & (0 \leq \varphi \leq \pi), \\ e^{-in_2\varphi} & (\pi \leq \varphi \leq 2\pi), \end{cases} \quad (1)$$

with integers n_1 and n_2 . Then, one notices that $n_1 - n_2$ must be an even integer such that Δ_s be nonzero everywhere; if $n_1 - n_2$ is an odd integer, $\lim_{\varphi \rightarrow \pi+0}\Delta_s$ and $\lim_{\varphi \rightarrow \pi-0}\Delta_s$ take opposite signs, so that $|\Delta| = 0$ at $\varphi = \pi$. The free-energy density f_1 (f_2) and the SC current \mathbf{j}_1 (\mathbf{j}_2) in the upper (lower) arm are expressed as

$$\begin{aligned} f_l &= \alpha|\Delta|^2 + \beta|\Delta|^4 + |\Delta|^2\frac{K}{R^2}\left(n_l - \frac{\Phi}{\Phi_0}\right)^2, \\ \mathbf{j}_l &= (-1)^l 4|e|K|\Delta|^2\frac{1}{R}\left(n_l - \frac{\Phi}{\Phi_0}\right)\hat{\varphi}, \end{aligned} \quad (2)$$

where the additional minus sign enters in \mathbf{j}_1 as it is defined in the clockwise direction in Fig. 1(b). The total free-energy density f_{GL} and the total bias current \mathbf{j}_{tot} are given by $f_{\text{GL}} = (f_1 + f_2)/2$ and $\mathbf{j}_{\text{tot}} = \mathbf{j}_1 + \mathbf{j}_2$.

Now, we calculate the critical bias current j_c inside the SC phase at $T < T_{c0}$, i.e., $\alpha < 0$, in the same procedure as that to derive the critical current in one dimension $j_c^{(\text{1D})}$ [4]. Since the amplitude of the SC gap function $|\Delta|$ is determined from the

condition $\frac{\delta f_{\text{GL}}}{\delta|\Delta|} = 0$ as

$$\begin{aligned} |\Delta|^2 &= \frac{-1}{2\beta} \left[\alpha + \frac{K}{2R^2} \left\{ \left(n_1 - \frac{\Phi}{\Phi_0} \right)^2 + \left(n_2 - \frac{\Phi}{\Phi_0} \right)^2 \right\} \right] \\ &= \frac{-1}{2\beta} \left[\alpha + \frac{K}{R^2} \left\{ \left(n_2 - \frac{n_{\text{tot}}}{2} - \frac{\Phi}{\Phi_0} \right)^2 + \frac{n_{\text{tot}}^2}{4} \right\} \right] \end{aligned} \quad (3)$$

with $n_{\text{tot}} = n_2 - n_1$, \mathbf{j}_{tot} is expressed as

$$|\mathbf{j}_{\text{tot}}| = \frac{2|e|K}{\beta R} \left[|\alpha| - \frac{K}{R^2} \left\{ \left(n_2 - \frac{n_{\text{tot}}}{2} - \frac{\Phi}{\Phi_0} \right)^2 + \frac{n_{\text{tot}}^2}{4} \right\} \right] |n_{\text{tot}}|. \quad (4)$$

Then, j_c is obtained as the maximum value of $|\mathbf{j}_{\text{tot}}|$ as a function of integers n_1 and n_2 under the constraint of $n_{\text{tot}} = n_2 - n_1 = \text{even integer}$, or equivalently, arbitrary integers n_2 and $n_{\text{tot}}/2$. Figure 1(d) shows a typical example of the calculated j_c as a function of Φ , where j_c is normalized by $j_0 = N(0)T_{c0}|e|v_F$. Among j_c 's for various combinations of n_1 and n_2 , the largest one gives the physical critical current which is indicated by a dotted curve in Fig. 1(d). One can see the LP oscillation in j_c similar to that in T_c .

In Refs. [6,7], j_c is derived in a different way, where it is assumed that the bias current is split equally into two and one arm with a larger net current consisting of the bias and additional circulating currents [suppose that it is, for example, the upper arm in Fig. 1(b)] determines j_c by the condition $|\mathbf{j}_1| = j_c^{(\text{1D})}$, leading to j_c showing a triangle-wave function of Φ . In the opposite arm, however, $|\mathbf{j}_2| < j_c^{(\text{1D})}$ should be satisfied because the circulating current cancels the bias current, so that the half of the system remains SC. In contrast, j_c obtained from Eq. (4) [see Fig. 1(d)] determines the SC instability over the whole system. In Al rings, the LP oscillation in j_c , which looks rather similar to Fig. 1(d), has been observed [5,6], validating the present approach, although its detailed structure depends on ring asymmetries [6]. In Nb rings, the j_c oscillation has been observed as the LP oscillation in the resistivity [12], and for a specific ring shape, vortex penetrations seem to affect j_c [7].

Spin-triplet p -wave case. Next, we will discuss the spin-triplet case where the gap function is expressed as

$$\hat{\Delta}_t = \begin{pmatrix} \Delta_{\uparrow\uparrow} & \Delta_{\uparrow\downarrow} \\ \Delta_{\downarrow\uparrow} & \Delta_{\downarrow\downarrow} \end{pmatrix} = \begin{pmatrix} -d_x + id_y & d_z \\ d_z & d_x + id_y \end{pmatrix}, \quad (5)$$

with the \mathbf{d} vector $\mathbf{d} = (d_x, d_y, d_z)$. In a magnetic field, the $\uparrow\downarrow$ Cooper pair becomes unfavorable, so that the \mathbf{d} vector tends to orient perpendicularly to the field, i.e., $d_z = 0$. For the ring geometry without the bias current, the \mathbf{d} vector can be expressed with the use of two winding numbers m and n as

$$\mathbf{d} = \left[\frac{|\Delta_{\uparrow\uparrow}|}{\sqrt{2}} \hat{d}^+ e^{-im\varphi} + \frac{|\Delta_{\downarrow\downarrow}|}{\sqrt{2}} \hat{d}^- e^{im\varphi} \right] e^{-in\varphi}, \quad (6)$$

where $\hat{d}^\pm = \frac{1}{\sqrt{2}}(\hat{x} \pm i\hat{y})$. To grasp the physical meanings of m and n , it is convenient to consider the simplified case of $|\Delta| = |\Delta_{\uparrow\uparrow}| = |\Delta_{\downarrow\downarrow}|$ where Eq. (6) is reduced to $\mathbf{d} = |\Delta|e^{-in\varphi}[\hat{x}\cos(m\varphi) + \hat{y}\sin(m\varphi)]$. It is clear that n is the phase winding number, whereas m describes the rotation of the \mathbf{d} vector along the circumference of the ring. In the case of $m = 0$, the \mathbf{d} vector is spatially uniform and n takes an integer value as in the spin-singlet case. For $m \neq 0$, on the other hand, n and m can take half-integer values as well as integer

values. Since the gap function should be single valued, n must be a half integer for a half-integer value of m to avoid the sign change at the two equivalent points of $\varphi = 0$ and 2π . This half-integer state accompanied with the **d**-vector rotation corresponds to the so-called half-quantum vortex which has often been discussed in the context of superfluid ^3He [13–16].

In the spin-triplet superconductor with the isotropic p -wave pairing interaction, the **d** vector is expressed as $d_\mu = \sum_i A_{\mu,i} \hat{p}_i$ with the order parameter $A_{\mu,i}$, and the GL free energy is given by $\mathcal{F}_{\text{GL}} = \int d\mathbf{r} [f^{(2)} + \delta f^{(2)} + f^{(4)}]$ with

$$f^{(2)} = \sum_{\mu,i,j} A_{\mu,i}^* \left[\frac{\alpha}{3} \delta_{i,j} A_{\mu,j} + K' (\Pi_j \Pi_j A_{\mu,i} + 2 \Pi_i \Pi_j A_{\mu,j}) \right],$$

$$\delta f^{(2)} = -\frac{\delta\alpha}{3} i \sum_i (A_{x,i} A_{y,i}^* - A_{y,i} A_{x,i}^*),$$

$$f^{(4)} = \sum_{\mu,\nu,i,j} [\beta_1 |A_{\mu,i} A_{\mu,i}|^2 + \beta_2 (A_{\mu,i}^* A_{\mu,i})^2 + \beta_3 A_{\mu,i}^* A_{\nu,i} A_{\nu,i}^* A_{\mu,j} \times A_{\nu,j} + \beta_4 A_{\mu,i}^* A_{\nu,i} A_{\nu,i}^* A_{\mu,j} + \beta_5 A_{\mu,i}^* A_{\nu,i} A_{\nu,i}^* A_{\mu,j}]. \quad (7)$$

This functional form is obtained from \mathcal{F}_{GL} for superfluid ^3He by replacing $-i\nabla$ with $\mathbf{\Pi}$, so that the coefficients are given by $-2\beta_1 = \beta_2 = \beta_3 = \beta_4 = -\beta_5 = 2\beta_0$ with $\beta_0 = \frac{7\xi(3)N(0)}{240\pi^2 T^2}$ and $K' = \frac{1}{5}N(0)(\frac{T_0}{T})^2 \xi_0^2$ in the weak-coupling limit [17]. The $\delta f^{(2)}$ term originates from the difference in the density of states between the up-spin and down-spin Fermi surfaces and thereby is active only in a magnetic field [17,18]. Within a linear approximation, we could express $\delta\alpha$ as $\delta\alpha = N(0)\eta\frac{\Phi}{\Phi_0}$. The SC current $\mathbf{j} = -\frac{\delta\mathcal{F}_{\text{GL}}}{\delta\mathbf{A}}$ is given by $j_\alpha = -4|e|K' \sum_{\mu,i,j} A_{\mu,i}^* (\delta_{ij}\Pi_\alpha + \delta_{\alpha j}\Pi_i + \delta_{\alpha i}\Pi_j) A_{\mu,j}$. Now, we consider a possible form of $A_{\mu,i}$ for the ring geometry. For simplicity, we assume that the spin and orbital degrees of freedom are decoupled such that $A_{\mu,i} = a_\mu w_{\mathbf{p},i}$, and take an axially symmetric orbital state of the form $w_{\mathbf{p},i} = \frac{1}{\sqrt{2}}(\hat{p}_x + i\hat{p}_y)_i$. We note that even if the polar state of the axially symmetric form $w_{\mathbf{p},i} = \hat{p}_{z,i}$ is assumed, the following discussion is essentially the same except the overall prefactors, so that the chiral nature of the orbital pairing state is not important.

Concerning the spin degrees of freedom a_μ , Eq. (6) can be straightforwardly extended to the case with the bias current, and a_μ can be expressed as

$$a_\mu = \begin{cases} \left[\frac{|\Delta_{\uparrow\uparrow}|}{\sqrt{2}} \hat{d}_\mu^+ e^{-im_1\varphi} + \frac{|\Delta_{\downarrow\downarrow}|}{\sqrt{2}} \hat{d}_\mu^- e^{im_1\varphi} \right] e^{-in_1\varphi} & (0 \leq \varphi \leq \pi), \\ \left[\frac{|\Delta_{\uparrow\uparrow}|}{\sqrt{2}} \hat{d}_\mu^+ e^{-im_2\varphi} + \frac{|\Delta_{\downarrow\downarrow}|}{\sqrt{2}} \hat{d}_\mu^- e^{im_2\varphi} \right] e^{-in_2\varphi} & (\pi \leq \varphi \leq 2\pi). \end{cases}$$

As in the spin-singlet case, there exists a constraint on n_1 , n_2 , m_1 , and m_2 such that $|\Delta_{\uparrow\uparrow}|$ and $|\Delta_{\downarrow\downarrow}|$ be nonzero even at the intersections between the upper and lower arms, namely, at $\varphi = 0$ and π ; $n_1 - n_2$ must be an even (odd) integer when $m_1 - m_2$ is an even (odd) integer, which is summarized in Table I. In Table I, type I represents the $m_1 = m_2 = 0$ state where the **d** vector is spatially uniform [see Fig. 2(a)], whereas types II and III represent the states with $m_1 \neq 0$ and/or $m_2 \neq 0$

TABLE I. Constraint on the phase winding numbers n_1 and n_2 and the **d**-vector winding numbers m_1 and m_2 .

Type	n_1, n_2	m_1, m_2	$n_1 - n_2$	$m_1 - m_2$
I	Integer	$m_1 = m_2 = 0$	Even	0
II	Integer	Integer $\neq 0$	Even	Even
			Odd	Odd
III	Half integer	Half integer	Even	Even
			Odd	Odd

where the **d** vector forms a texture along the circumference [see Figs. 2(b) and 2(c)]. In the type-II (type-III) state, n_1 , n_2 , m_1 , and m_2 are integers (half integers), and thus, as illustrated in Fig. 2(b) [Fig. 2(c)], the **d** vectors at $\varphi = 0$ and 2π are parallel (antiparallel) to each other.

By substituting $A_{\mu,i} = a_\mu w_{\mathbf{p},i}$ into Eq. (7), we obtain the total free-energy density $f_{\text{GL}} = (f_1 + f_2)/2$ as

$$f_{\text{GL}} = \frac{1}{2} \sum_{\sigma=\uparrow,\downarrow} \left\{ \frac{\alpha - \epsilon_\sigma \delta\alpha}{3} |\Delta_{\sigma\sigma}|^2 + 2\beta_0 |\Delta_{\sigma\sigma}|^4 + \frac{K'}{R^2} |\Delta_{\sigma\sigma}|^2 \times \left[\left(n_1 + \epsilon_\sigma m_1 - \frac{\Phi}{\Phi_0} \right)^2 + \left(n_2 + \epsilon_\sigma m_2 - \frac{\Phi}{\Phi_0} \right)^2 \right] \right\}, \quad (8)$$

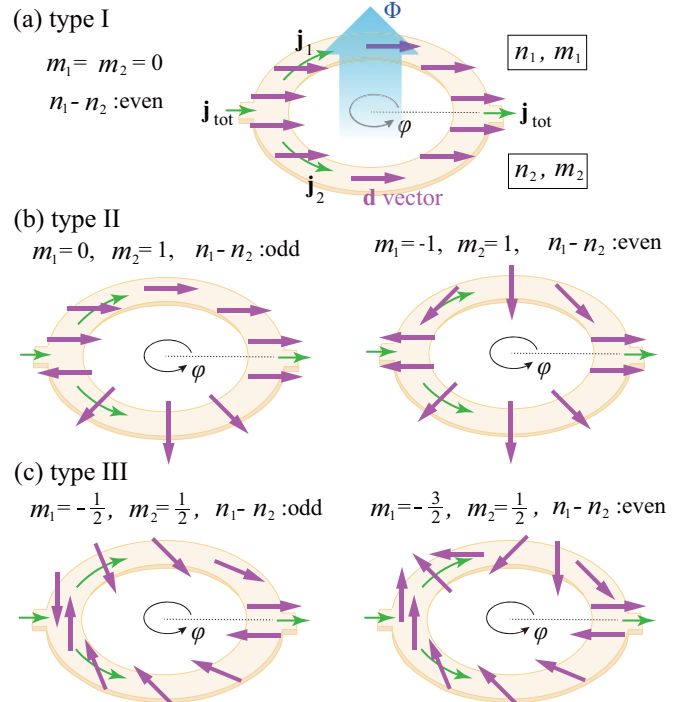


FIG. 2. Schematically drawn **d**-vector textures in the spin-triplet SC ring in the presence of both the magnetic flux Φ and the bias current \mathbf{j}_{tot} , where a magenta arrow represents the **d** vector and $|\Delta_{\uparrow\uparrow}| = |\Delta_{\downarrow\downarrow}|$ is assumed for ease of understanding. (a) Type-I state with $m_1 = m_2 = 0$, (b) type-II states with $m_1 = 0$ and $m_2 = 1$ (left) and $m_1 = -1$ and $m_2 = 1$ (right), and (c) type-III states with $m_1 = -\frac{1}{2}$ and $m_2 = \frac{1}{2}$ (left) and $m_1 = -\frac{3}{2}$ and $m_2 = \frac{1}{2}$ (right), which are categorized in Table I.

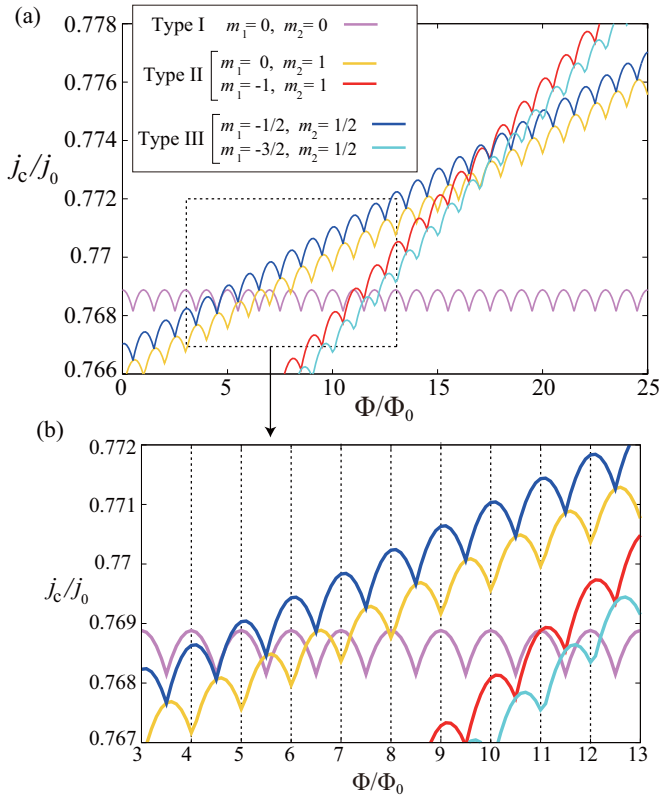


FIG. 3. LP oscillation in j_c obtained at $T/T_{c0} = 0.6$ for the spintriplet p -wave ring with $R/\xi_0 = 50$ and $\eta = 0.004$. (a) j_c 's for the five types of \mathbf{d} -vector textures shown in Fig. 2; violet (type I with $m_1 = m_2 = 0$), yellow (type II with $m_1 = 0, m_2 = 1$), red (type II with $m_1 = -1, m_2 = 1$), blue (type III with $m_1 = -\frac{1}{2}, m_2 = \frac{1}{2}$), and cyan (type III with $m_1 = -\frac{3}{2}, m_2 = \frac{1}{2}$). A zoomed view of the region enclosed by a dotted box is shown in (b). In (b), dashed lines indicate peak positions of the LP oscillation for the type-I state realized at low fields.

where $\epsilon_{\uparrow(\downarrow)} = 1(-1)$. In the same manner, the total current $\mathbf{j}_{\text{tot}} = \mathbf{j}_1 + \mathbf{j}_2$ is calculated as

$$\mathbf{j}_{\text{tot}} = -\hat{\varphi} \frac{4|e|K'}{R} [(|\Delta_{\uparrow\uparrow}|^2 + |\Delta_{\downarrow\downarrow}|^2)(n_1 - n_2) + (|\Delta_{\uparrow\uparrow}|^2 - |\Delta_{\downarrow\downarrow}|^2)(m_1 - m_2)], \quad (9)$$

with

$$|\Delta_{\sigma\sigma}|^2 = \frac{-1}{4\beta_0} \left\{ \frac{\alpha - \epsilon_\sigma \delta\alpha}{3} + \frac{K'}{R^2} \left[\left(n_1 + \epsilon_\sigma m_1 - \frac{\Phi}{\Phi_0} \right)^2 + \left(n_2 + \epsilon_\sigma m_2 - \frac{\Phi}{\Phi_0} \right)^2 \right] \right\}, \quad (10)$$

where Eq. (10) is obtained from the conditions $\frac{\delta f_{\text{GL}}}{\delta |\Delta_{\uparrow\uparrow}|} = 0$ and $\frac{\delta f_{\text{GL}}}{\delta |\Delta_{\downarrow\downarrow}|} = 0$. The maximum value of $|\mathbf{j}_{\text{tot}}|$ as a function of $n_1, n_2, m_1,$ and m_2 under the constraints shown in Table I corresponds to j_c .

Figure 3 shows the calculation result for $R/\xi_0 = 50$, $T/T_{c0} = 0.6$, and $\eta = 0.004$. As one can see from Fig. 3(a), j_c for the type-I state (violet curve) exhibits the conventional

LP oscillation, whereas j_c 's for the type-II (red and yellow curves) and type-III (blue and cyan curves) states are increasing functions of Φ accompanied with the LP oscillation. The largest critical current is given by the type-I state at low fields, whereas at higher fields, it is given by the type-II or type-III state with $|m_1| = |m_2| \neq 0$ [blue or red curve in Fig. 2(a)], suggesting that the transition between the uniform and textured \mathbf{d} -vector configurations occurs. In Fig. 3, j_c 's for $|m_1| \neq |m_2|$ (yellow and cyan curves) are always smaller than j_c 's for $|m_1| = |m_2|$ (red and blue curves) except at the degenerate points, so that the $|m_1| \neq |m_2|$ states are not realized, at least within the realm of this theory.

As one can see from the zoomed view shown in Fig. 3(b), the phase of the LP oscillation in the physical critical current, i.e., the largest j_c , remains unchanged without showing a half-quantum shift, even after the transition into the type-III state with the \mathbf{d} -vector texture (compare the violet and blue curves). In the case of $m_1 = 0$ and $m_2 = 1$ (see a yellow curve), on the other hand, the oscillation pattern is half-quantum shifted compared with the low-field conventional LP oscillation, although such a half-quantum-shifted state with $|m_1| \neq |m_2|$ is unstable.

Now, we discuss why the \mathbf{d} -vector texture yields the larger j_c in the presence of the magnetic field. In Eq. (9), one notices that \mathbf{j}_{tot} consists of two parts: One is a phase-gradient current proportional to $n_1 - n_2$, and the other is a \mathbf{d} -vector-texture-induced one proportional to $m_1 - m_2$. In the type-I state with $m_1 = m_2 = 0$, \mathbf{j}_{tot} is governed only by the former which is coupled to $|\Delta_{\uparrow\uparrow}|^2 + |\Delta_{\downarrow\downarrow}|^2$. Since the effect of the Zeeman splitting, $\pm\delta\alpha$, is completely canceled out in $|\Delta_{\uparrow\uparrow}|^2 + |\Delta_{\downarrow\downarrow}|^2$ [see Eq. (10)], j_c for the type-I state is field independent except for the LP oscillation. In contrast, in the type-II and type-III states with $m_1 - m_2 \neq 0$, the latter \mathbf{d} -vector-texture term is active, being coupled to $|\Delta_{\uparrow\uparrow}|^2 - |\Delta_{\downarrow\downarrow}|^2$ which is roughly proportional to $\delta\alpha = \eta \frac{\Phi}{\Phi_0}$, so that j_c increases with increasing field. Since the \mathbf{d} -vector texture itself costs the gradient energy, the type-II and type-III states are unstable at zero field, but with increasing field, their j_c 's are elevated by the \mathbf{d} -vector-texture term proportional to both $m_1 - m_2$ and $\eta \frac{\Phi}{\Phi_0}$, eventually overwhelming the type-I value. Thus, in a system with a larger Fermi-surface Zeeman splitting η , the transition between the type-I and type-III states occurs at a lower field.

The above discussion on j_c can be understood from the viewpoint of the free energy. With the use of $n_{\text{tot}} = n_2 - n_1$, the gradient energy in Eq. (8) can be rewritten as

$$\frac{K'}{R^2} (|\Delta_{\uparrow\uparrow}|^2 + |\Delta_{\downarrow\downarrow}|^2) \left[\left(n_2 - \frac{n_{\text{tot}}}{2} - \frac{\Phi}{\Phi_0} + \lambda \frac{m_1 + m_2}{2} \right)^2 + \frac{n_{\text{tot}}^2}{4} + \frac{m_1^2}{2} + \frac{m_2^2}{2} - \lambda n_{\text{tot}} \frac{m_1 - m_2}{2} - \left(\lambda \frac{m_1 + m_2}{2} \right)^2 \right],$$

with $\lambda = \frac{|\Delta_{\uparrow\uparrow}|^2 - |\Delta_{\downarrow\downarrow}|^2}{|\Delta_{\uparrow\uparrow}|^2 + |\Delta_{\downarrow\downarrow}|^2}$. Due to the $-\lambda n_{\text{tot}} (m_1 - m_2)$ term, which is active in the presence of both the bias current \mathbf{j}_{tot} roughly proportional to $n_{\text{tot}} \neq 0$, and the Zeeman splitting, i.e., $\lambda \propto \eta \frac{\Phi}{\Phi_0} \neq 0$, the \mathbf{d} -vector texture with $m_1 - m_2 \neq 0$ can acquire a larger energy gain than the energy cost of $m_1^2 + m_2^2$, leading to the occurrence of type-II and type-III states. We

note that such a linear coupling between the magnetic field and the SC current occurs in the different context of noncentrosymmetric superconductors [19] where the coupling yields a phase-modulated helical SC state and associated magnetoelectric phenomena [20–27].

Discussion. In this Letter, we have demonstrated that in the spin-triplet SC ring, the critical bias current exhibits the LP oscillation, being accompanied by the field-induced transition into the textured state of the \mathbf{d} vector. Here, we comment on additional effects which are not incorporated in the present GL analysis. First, we have assumed the discontinuous change in winding numbers at the intersections between the upper and lower arms whose gradient energy may suppress the stability of the textured state. Such an additional energy cost, however, could be estimated by using the functional form near $\varphi = 0$, $a_\mu = |\Delta_{\sigma\sigma}|e^{-im(\varphi)\varphi}$ with $m(\varphi) = \frac{1}{2}[m_1 + m_2 + (m_1 - m_2)\tanh(\varphi/L_0)]$ and $L_0 = \xi_0/R$, as $\int_{-L_0}^{L_0} K'|\nabla a_\mu|^2 d\varphi \sim \frac{K'}{R^2}|\Delta_{\sigma\sigma}|^2 \frac{\xi_0}{R}$, so that for a relatively large ring radius, it should be irrelevant compared with the energy gain $-\frac{K'}{R^2}|\Delta_{\sigma\sigma}|^2 \lambda n_{\text{tot}}(m_1 - m_2)$ to stabilize the \mathbf{d} -vector texture. Second, although our analysis is based on the weak-coupling BCS theory, the Fermi-liquid correction may assist the \mathbf{d} -vector texture as in the case of superfluid ^3He [13,16,18]. Third, we have assumed that the spin space is isotropic and the \mathbf{d} vector can rotate freely, but in real

materials, the \mathbf{d} vector may be subject to pinning due to, for example, magnetic impurities.

In the presence of the \mathbf{d} -vector pinning, when the field is gradually increased in the initial uniform state shown in Fig. 2(a), the type-II state possessing the half-uniform and half-textured \mathbf{d} -vector configuration shown in the left panel of Fig. 2(b) might possibly be realized with the \mathbf{d} vector in the upper arm being pinned to be almost uniform, instead of the theoretically expected type-III state with the fully textured \mathbf{d} -vector configuration shown in the left panel of Fig. 2(c). If it happens, a switching from the usual LP oscillation to the half-quantum-shifted one [see the yellow curve in Fig. 3(b)] should be observed, being distinguished from the domain-induced unconventional LP pattern which is half-quantum shifted from the beginning [8,28]. Although such a field-induced half-quantum shift has yet to be reported even in the LP experiments conducted for the spin-triplet candidate Sr_2RuO_4 [29–32] (its pairing symmetry is still controversial [33]), we believe that our result presented here will promote the exploration and further understanding of not only spin-triplet but also various classes of superconductors.

Acknowledgments The author thanks M. Tokuda and Y. Niimi for stimulating discussions and T. Mizushima, R. Ikeda, and M. Sigrist for valuable comments. This work is partially supported by JSPS KAKENHI Grant No. JP21K03469.

-
- [1] W. A. Little and R. D. Parks, *Phys. Rev. Lett.* **9**, 9 (1962).
 [2] R. D. Parks and W. A. Little, *Phys. Rev.* **133**, A97 (1964).
 [3] R. P. Groff and R. D. Parks, *Phys. Rev.* **176**, 567 (1968).
 [4] M. Thinkham, *Introduction to Superconductivity*, 2nd ed. (Dover, New York, 1996), Chap. 4.
 [5] V. L. Gurtovoi, S. V. Dubonos, S. V. Karpi, A. V. Nikulov, and V. A. Tulin, *J. Exp. Theor. Phys.* **105**, 262 (2007).
 [6] V. L. Gurtovoi, A. I. Ilin, and A. V. Nikulov, *Phys. Lett. A* **384**, 126669 (2020).
 [7] S. Michotte, D. Lucot, and D. Mailly, *Phys. Rev. B* **81**, 100503(R) (2010).
 [8] Y. Li, X. Xu, M.-H. Lee, M.-W. Chu, and C. L. Chien, *Science* **366**, 238 (2019).
 [9] N. R. Werthamer, in *Superconductivity*, edited by R. D. Parks (Dekker, New York, 1969), p. 321.
 [10] K. Aoyama, R. Beard, D. E. Sheehy, and I. Vekhter, *Phys. Rev. Lett.* **110**, 177004 (2013).
 [11] Z. J. Ying, M. Cuoco, C. Ortix, and P. Gentile, *Phys. Rev. B* **96**, 100506(R) (2017).
 [12] M. Tokuda, R. Nakamura, M. Maeda, and Y. Niimi, *Jpn. J. Appl. Phys.* **61**, 060908 (2022).
 [13] M. M. Salomaa and G. E. Volovik, *Phys. Rev. Lett.* **55**, 1184 (1985).
 [14] S. Autti, V. V. Dmitriev, J. T. Mäkinen, A. A. Soldatov, G. E. Volovik, A. N. Yudin, V. V. Zavjalov, and V. B. Eltsov, *Phys. Rev. Lett.* **117**, 255301 (2016).
 [15] J. A. Sauls, *Physics* **9**, 148 (2016).
 [16] N. Nagamura and R. Ikeda, *Phys. Rev. B* **98**, 094524 (2018).
 [17] D. Volhardt and P. Wolfle, *The Superfluid Phases of Helium 3* (Taylor and Francis, London, 1990).
 [18] V. Vakaryuk and A. J. Leggett, *Phys. Rev. Lett.* **103**, 057003 (2009).
 [19] *Non-Centrosymmetric Superconductors: Introduction and Overview*, edited by E. Bauer and M. Sigrist, Lecture Notes in Physics Vol. 847 (Springer, Berlin, 2012).
 [20] V. M. Edelstein, *Phys. Rev. Lett.* **75**, 2004 (1995).
 [21] V. M. Edelstein, *Sov. Phys. JETP* **68**(6), 1244 (1989); S. K. Yip, *Phys. Rev. B* **65**, 144508 (2002).
 [22] O. V. Dimitrova and M. V. Feigel'man, *JETP Lett.* **78**, 637 (2003).
 [23] K. V. Samokhin, *Phys. Rev. B* **70**, 104521 (2004).
 [24] R. P. Kaur, D. F. Agterberg, and M. Sigrist, *Phys. Rev. Lett.* **94**, 137002 (2005).
 [25] S. Fujimoto, *Phys. Rev. B* **72**, 024515 (2005).
 [26] K. Aoyama and M. Sigrist, *Phys. Rev. Lett.* **109**, 237007 (2012).
 [27] K. Aoyama, L. Savary, and M. Sigrist, *Phys. Rev. B* **89**, 174518 (2014).
 [28] X. Xu, Y. Li, and C. L. Chien, *Phys. Rev. Lett.* **124**, 167001 (2020).
 [29] X. Cai, Y. A. Ying, N. E. Staley, Y. Xin, D. Fobes, T. J. Liu, Z. Q. Mao, and Y. Liu, *Phys. Rev. B* **87**, 081104(R) (2013).
 [30] Y. Yasui, K. Lahabi, M. S. Anwar, Y. Nakamura, S. Yonezawa, T. Terashima, J. Aarts, and Y. Maeno, *Phys. Rev. B* **96**, 180507(R) (2017).
 [31] Y. Yasui, K. Lahabi, V. F. Becerra, R. Fermin, M. S. Anwar, S. Yonezawa, T. Terashima, M. V. Milosevic, J. Aarts, and Y. Maeno, *npj Quantum Mater.* **5**, 21 (2020).
 [32] X. Cai, B. Zakrzewski, Y. A. Ying, H.-Y. Kee, M. Sigrist, J. E. Ortmann, W. Sun, Z. Mao, and Y. Liu, *arXiv:2010.15800*.
 [33] A. Pustogow, Y. Luo, A. Chronister, Y.-S. Su, D. A. Sokolov, F. Jerzembeck, A. P. Mackenzie, C. W. Hicks, N. Kikugawa, S. Raghu, E. D. Bauer, and S. E. Brown, *Nature (London)* **574**, 72 (2019).